A MIXED SPECTRAL DOMAIN METHOD APPLIED TO THE ANALYSIS OF GENERALIZED DIELECTRIC-LOADED RIDGED WAVEGUIDES

K.T. Ng* and C.H. Chan**

*** Dept. of Elec. Eng., University of Virginia, Charlottesville, VA 22901**
**** Dept. of Elec. & Computer Eng., University of Illinois, Urbana, IL 61801**

ABSTRACT

A new mixed spectral domain method is applied for the analysis of generalized dielectric-loaded ridged waveguides. Auxillary structures are constructed for formulating the spectral Green's functions and applying the spectral immittance method. Magntic surface currents at apertures are identified as unknowns. Mixing different spectral domains existing on the two sides of an aperture in a spectral Galerkin approach leads to the characteristic equations required for the dispersion analysis. Representative results are obtained to illustrate the application of the method.

I. INTRODUCTION

Conventional ridged waveguide and its variations have found many applications in microwave and millimeter-wave devices [1]-[6]. They allow wave propagation with smaller overall guide dimensions than those required in rectangular waveguides. In addition, ridged waveguides offer the advantages of large bandwidths, low characteristic impedances, and the possibility of integrated circuit designs [3].

Since the original ridged waveguide structure was proposed, different variations, including dielectric loading, have been made to control its propagation characteristics [7]. In this paper a general mixed spectral domain technique will be developed and used to analyze a class of dielectric-loaded ridged waveguides shown in Fig. 1. These structures have been analyzed separately before with analytical approximations, mode matching techniques, variational techniques, and Method of Moments [7]-[10]. Compared to these previous methods, the technique developed in this paper is more versatile and numerically efficient.

The spectral domain method, using a generalized immittance approach [11], is popular for the analysis of planar and quasi-planar structures. It offers simple formulation and high numerical efficiency . With a proper choice of basis functions, only a small number of them is required, leading to a small matrix size. The conventional spectral domain immittance approach, however, cannot be applied directly to analyze the structures shown in Fig. 1. This is because the Fourier transform variable α in x will have different values for different regions, in order to satisfy the boundary conditions on the side walls, which have different separations in different regions. As a result, a new mixed domain approach is developed, which maintains the advantages of the spectral domain immittance method. The approach is general and can be applied to analyze other structures consisting of variations in side wall separations, e.g., fin-lines with grooves.

II. FORMULATION

As an illustration of the formulation, the slotted, dielectrically loaded ridged waveguide in Fig. 1(c) will be considered. Because of the symmetry, as shown in Fig. 2(a), only half of the original structure needs to be considered, with a magnetic wall at y=0. The spectral domain immittance approach can then be used for the equivalent structures shown in Fig. 2(b). In Fig. 2(b), following the equivalence principle [12], apertures are replaced by perfectly conducting planes and appropriate magnetic surface currents are used to restore the fields. The total transverse (to y) magnetic field at $y=d_1^+$ is radiated by magnetic surface current $\overline{M}_1$ in the presence of the conducting plane and the environment for $y>d_1$. On the other hand, the transverse magnetic field at $y=d_1^-$ and $y=d_2^+$ are radiated by magnetic surface currents $-\overline{M}_1$ and $\overline{M}_2$ in the presence of the shorted apertures. Finally, the magnetic field at $y=d_2^-$ is due to $-\overline{M}_2$ radiating in the presence of the conducting plane and the environment for $y<d_2$. One can use the conventional spectral domain immittance approach to easily derive the spectral dyadic Green's functions for the equivalent structures. Enforcement of continuity of the transverse magnetic fields across the apertures allows one to relate $\overline{M}_1$ and $\overline{M}_2$.

The spectral Galerkin method is then applied by expanding the unknown magnetic surface currents with sets of known basis functions provided in [13], weighted with unknown coefficients. The Fourier transforms of these basis functions are functions of zero-order Bessel functions of the first kind, sampled at different intervals. Further these functions provide a singularity behavior of $x^{-1/2}$ at the edges of the apertures for the z components of $\overline{M}_1$ and $\overline{M}_2$. Theoretically the edge singularity of the aperture fields behave as $x^{-1+\lambda}$ rather than as $x^{-1/2}$, where λ can be determined from the formula provided in [14]. In order to incorporate the exact edge singularity behavior, the square root appearing in these basis functions needs to be replaced by a $(1-\lambda)$ -th root. However, this will make the Fourier transforms of the basis functions more difficult to evaluate. As numerical experiments have shown that there is no significant differences in the calculated dispersion characteristics whether the square root or $(1-\lambda)$ -th root is used, the square root is chosen for the basis functions.

To determine the unknown weighting coefficients, the transverse magnetic fields at $y=d_1$ and $y=d_2$ are tested with the same basis functions for $\overline{M}_1$ and $\overline{M}_2$. One then obtains

$$2\pi/a \begin{bmatrix} \tilde{M}_{1x}\tilde{G}^1_{xx}\tilde{M}_{1x} & \tilde{M}_{1x}\tilde{G}^1_{xz}\tilde{M}_{1z} \\ \tilde{M}_{1z}\tilde{G}^1_{zx}\tilde{M}_{1x} & \tilde{M}_{1z}\tilde{G}^1_{zz}\tilde{M}_{1z} \end{bmatrix}_{\alpha_a} \begin{bmatrix} C_{M1x} \\ C_{M1z} \end{bmatrix} = \tag{1}$$

$$2\pi/b \begin{bmatrix} \tilde{M}_{1x}\tilde{G}^2_{xx}\tilde{M}_{1x} & \tilde{M}_{1x}\tilde{G}^2_{xz}\tilde{M}_{1z} \\ \tilde{M}_{1z}\tilde{G}^2_{zx}\tilde{M}_{1x} & \tilde{M}_{1z}\tilde{G}^2_{zz}\tilde{M}_{1z} \end{bmatrix}_{\alpha_b} \begin{bmatrix} C_{M1x} \\ C_{M1z} \end{bmatrix}$$

$$+ 2\pi/b \begin{bmatrix} \tilde{M}_{1x}\tilde{G}^3_{xx}\tilde{M}_{2x} & \tilde{M}_{1x}\tilde{G}^3_{xz}\tilde{M}_{2z} \\ \tilde{M}_{1z}\tilde{G}^3_{zx}\tilde{M}_{2x} & \tilde{M}_{1z}\tilde{G}^3_{zz}\tilde{M}_{2z} \end{bmatrix}_{\alpha_b} \begin{bmatrix} C_{M2x} \\ C_{M2z} \end{bmatrix}$$

$$2\pi/b \begin{bmatrix} \tilde{M}_{2x}\tilde{G}^4_{xx}\tilde{M}_{1x} & \tilde{M}_{2x}\tilde{G}^4_{xz}\tilde{M}_{1z} \\ \tilde{M}_{2z}\tilde{G}^4_{zx}\tilde{M}_{1x} & \tilde{M}_{2z}\tilde{G}^4_{zz}\tilde{M}_{1z} \end{bmatrix}_{\alpha_b} \begin{bmatrix} C_{M1x} \\ C_{M1z} \end{bmatrix} \tag{2}$$

$$+ 2\pi/b \begin{bmatrix} \tilde{M}_{2x}\tilde{G}^5_{xx}\tilde{M}_{2x} & \tilde{M}_{2x}\tilde{G}^5_{xz}\tilde{M}_{2z} \\ \tilde{M}_{2z}\tilde{G}^5_{zx}\tilde{M}_{2x} & \tilde{M}_{2z}\tilde{G}^5_{zz}\tilde{M}_{2z} \end{bmatrix}_{\alpha_b} \begin{bmatrix} C_{M2x} \\ C_{M2z} \end{bmatrix}$$

$$= 2\pi/c \begin{bmatrix} \tilde{M}_{2x}\tilde{G}^6_{xx}\tilde{M}_{2x} & \tilde{M}_{2x}\tilde{G}^6_{xz}\tilde{M}_{2z} \\ \tilde{M}_{2z}\tilde{G}^6_{zx}\tilde{M}_{2x} & \tilde{M}_{2z}\tilde{G}^6_{zz}\tilde{M}_{2z} \end{bmatrix}_{\alpha_c} \begin{bmatrix} C_{M2x} \\ C_{M2z} \end{bmatrix}$$

where C_{M1} and C_{M2} are the weighting coefficients for $\overline{M}_1$ and $\overline{M}_2$ (with both x and z components), $\tilde{G}$'s are the spectral Green's functions, and α_a, α_b, and α_c represent the discrete Fourier transform variables. Different factors, $2\pi/a$, $2\pi/b$, and $2\pi/c$, corresponding to different sampling intervals, occur because of the different spectral domains encountered. Also, it should be noted that the summations over all spectral terms as well as the basis functions are omitted in Eqs. (1)-(2) for simplicity. The propagation constant k_z is given by the eigenvalues of the combined matrix equations (1) and (2), which can then be solved for the unknown weighting coefficients. The fields and impedances can then be obtained.

Finally the dielectric-loaded single-ridged and double-ridged waveguides shown in Figs. 1(a) and 1(b) can be treated with a similar procedure. These structures have only one aperture, after symmetry is applied and a magnetic wall is inserted at the center. Hence, Eq. (2) is not required, and C_{M2x} and C_{M2z} should be set to zero in Eq. (1).

III. RESULTS

As an illustration of the versatility and validity of the method, numerical results on the normalized propagation constant for the dominant mode are obtained in Figs. 3-5 respectively for a dielectric-loaded single-ridged waveguide, a dielectric-loaded double-ridged waveguide, and a slotted, dielectrically loaded ridged waveguide. Three basis functions for each component of the magnetic surface current are used, and the Fourier transform variables are $\alpha_a=n\pi/a$, $\alpha_b=n\pi/b$, $\alpha_c=n\pi/c$. As one can see, the propagation characteristic can be greatly affected by dielectric loading. Comparison with previous numerical and experimental results are excellent.

IV. CONCLUSIONS

A simple and numerically efficient mixed spectral domain method has been presented for the analysis of generalized dielectric-loaded ridged waveguides. The formulation allows one to maintain the advantages of the spectral domain immittance approach in the more complicated structures, which requires mixing two different spectral domains on the two sides of an aperture. Representative results for different structures compare well with those obtained previously with different methods. This method appears to be suitable for efficient analysis of more complicated transmission structures which involve variations in the side-wall separations in a rectangular waveguide.

REFERENCES

1. S. Hopfer, "The design of ridged waveguides," IRE Trans. Microwave Theory Tech., vol. MTT-3, pp. 20-29, Oct. 1955.

2. A.M.K. Sadd, J.D. Miller, A. Mitha, and R. Brown, "Analysis of antipodal ridge waveguide structure and application on extremely wide stopband lowpass filter," in 1986 IEEE MTT-S Symp. Dig., pp. 361-363.

3. Y. Konishi, K. Uenakada, N. Yazawa, N. Hoshino, and T. Takahashi, "Simplified 12-GHz low-noise converter with mounted planar circuit in waveguide," IEEE Trans. Microwave Theory Tech., vol. MTT-22, pp. 451-454, Apr. 1974.

4. L.-P. Schmidt and H. Meinel, "Broadband millimeter-wave PIN-diode attenuator with double-ridged waveguide flanges," Electron. Lett., vol. 18, no. 19, pp. 839-840, Sept. 1982.

5. J. Bornemann and F. Arndt, "Modal-S-Matrix design of optimum stepped ridged and finned waveguide transformers," IEEE Trans. Microwave Theory Tech., vol. MTT-35, pp. 561-567, June 1987.

6. G.G. Mazumder and P.K. Saha, "A novel rectangular waveguide with double T-septums," IEEE Trans. Microwave Theory Tech., vol. MTT-33, pp. 1235-1238, Nov. 1985.

7. A.T. Villeneuve, "Analysis of slotted, dielectrically loaded, ridged waveguide," IEEE Trans. Microwave Theory Tech., vol. MTT-32, pp. 1302-1310, Oct. 1984.

8. T.S. Chen, "Calculations of the parameters of ridge waveguides," IRE Trans. Microwave Theory Tech., vol. MTT-5, pp. 12-17, Jan. 1957.

9. J.P. Montgomery, "On the complete eigenvalue solution of ridged waveguide," IEEE Trans. Microwave Theory Tech., vol. MTT-19, pp. 547-555, June 1971.

10. Y. Utsumi, "Variational analysis of ridged waveguide modes," IEEE Trans. Microwave Theory Tech., vol. MTT-33, pp. 111-120, Feb. 1985.

11. T. Itoh, "Spectral domain immitance approach for dispersion characteristics of generalized printed transmission lines," IEEE Trans. Microwave Theory Tech., vol. MTT-28, pp. 733-736, July 1980.

12. R.F. Harrington, *Time-Harmonic Electromagnetic Fields*. New York: McGraw-Hill, 1961.

13. E.G. Farr, C.H. Chan, and R. Mittra, "A frequency-dependent coupled-mode analysis of multiconductor microstrip lines with application to VLSI interconnection problems," IEEE Trans. Microwave Theory Tech., vol. MTT-34, pp. 307-310, Feb. 1986.

14. R. Mittra and S.W. Lee, *Analytical Techniques in the Theory of Guided Waves*. New York: Macmillan, 1971, pp. 4-11.

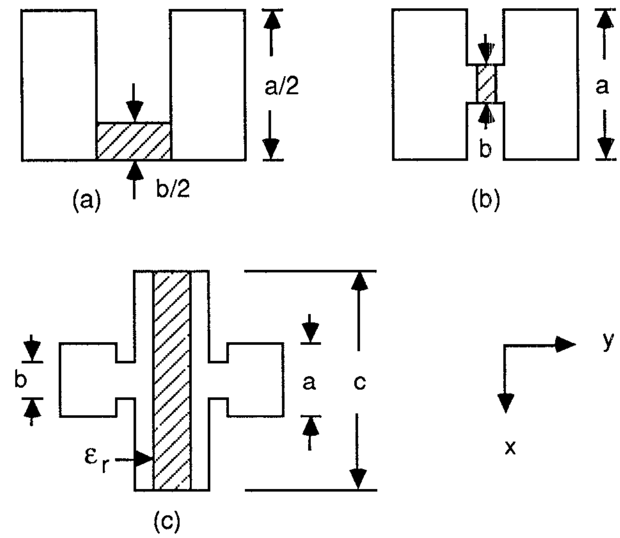

Fig. 1 A class of ridged waveguides. (a) Dielectric-loaded single-ridged waveguide. (b) Dielectric-loaded double-ridged waveguide. (c) Slotted dielectric-loaded ridged waveguide.

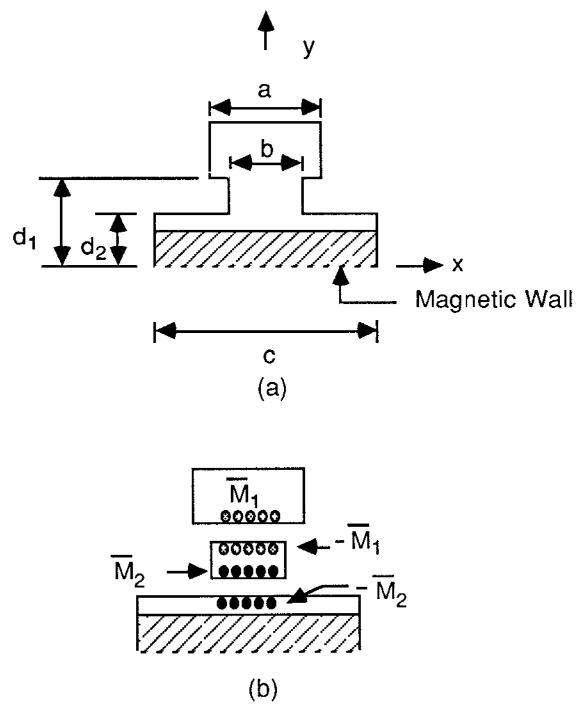

Fig. 2 Equivalent structures for the slotted dielectric-loaded ridged waveguide shown in Fig. 1(c). (a) Half of original structure, with magnetic wall at y=0. (b) Equivalent structures based on the equivalence principle.

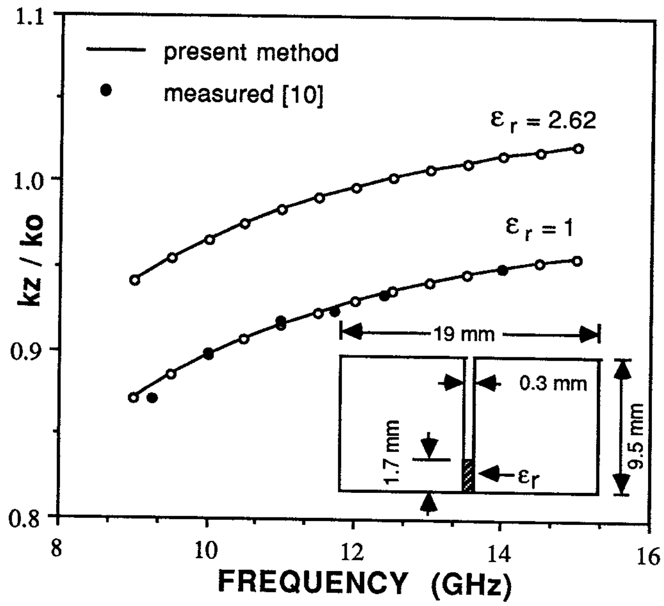

Fig. 3 Normalized propagation constant for dielectric-loaded single-ridged waveguides.

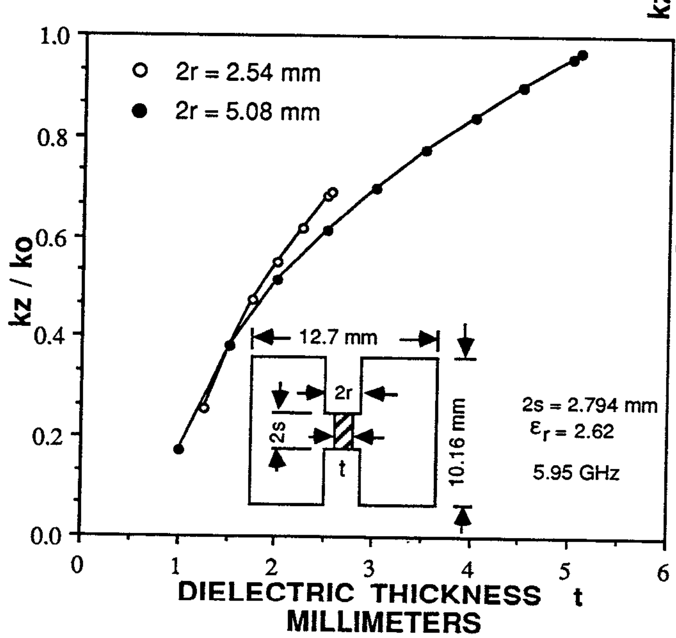

Fig. 4 Normalized propagation constant versus dielectric slab thickness for dielectric-loaded double-ridged waveguides.

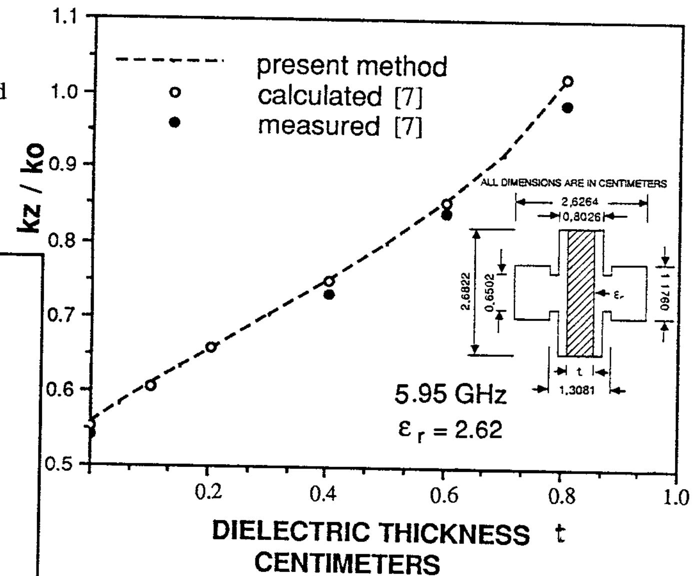

Fig. 5 Normalized propagation constant versus dielectric slab thickness for a slotted dielectric-loaded ridged waveguide.